Title: Disrupted brain gray matter connectome in social anxiety disorder: A novel individualized structural covariance network analysis

Running title: Disrupted brain gray matter connectome in SAD

Xun Zhang PhD[1,2,3,#], Han Lai PhD[4,#], Qingyuan Li PhD[1,2,3], Xun Yang PhD[5], Nanfang Pan PhD[1,2,3], Min He MM[1,2,3], Graham J. Kemp DSc[6], Song Wang PhD[1,2,3,*], Qiyong Gong MD, PhD[1,7,*]

Affiliations:

[1]Huaxi MR Research Center (HMRRC), Department of Radiology, West China Hospital of Sichuan University, Chengdu, Sichuan 610041, China

[2]Functional & Molecular Imaging Key Laboratory of Sichuan Province, West China Hospital of Sichuan University, Chengdu, Sichuan 610041, China

[3]Research Unit of Psychoradiology, Chinese Academy of Medical Sciences, Chengdu, Sichuan 610041, China

[4]Department of Psychology, Army Medical University, Chongqing 400044, China

[5]School of Public Affairs, Chongqing University, Chongqing 400044, China

[6]Liverpool Magnetic Resonance Imaging Centre (LiMRIC) and Institute of Life Course and Medical Sciences, University of Liverpool, Liverpool L69 3BX, UK

[7]Department of Radiology, West China Xiamen Hospital of Sichuan University, Xiamen, Fujian 361000, China

***Corresponding Authors**:

Song Wang, PhD., Huaxi MR Research Center (HMRRC), Department of Radiology, West China Hospital of Sichuan University, Chengdu, China. E-mail: wangs_psych@163.com

Qiyong Gong, MD, PhD, Department of Radiology, West China Xiamen Hospital of Sichuan University, Xiamen, China. E-mail: qiyonggong@hmrrc.org.cn

[#] Xun Zhang and Han Lai contributed equally to this study.

Abstract

Phenotyping approaches grounded in structural network science can offer insights into the neurobiological substrates of psychiatric diseases, but this remains to be clarified at the individual level in social anxiety disorder (SAD). Using a recently-developed approach combining probability density estimation and Kullback-Leibler divergence, we constructed single-subject structural covariance networks (SCNs) based on multivariate morphometry (cortical thickness, surface area, curvature, and volume), and quantified their global/nodal network properties using graph-theoretical analysis. We compared network metrics between SAD patients and healthy controls (HC) and analysed the relationship to clinical characteristics. We also used support vector machine analysis to explore the ability of graph-theoretical metrics to discriminate SAD patients from HC. Globally, SAD patients showed higher global efficiency, shorter characteristic path length, and stronger small-worldness. Locally, SAD patients showed abnormal nodal centrality mainly involving left superior frontal gyrus, right superior parietal lobe, left amygdala, right paracentral gyrus, right lingual, and right pericalcarine cortex. Altered topological metrics were associated with the symptom severity and duration. Graph-based metrics allowed single-subject classification of SAD versus HC with total accuracy of 78.7%. This finding, that the topological organization of SCN in SAD patients is altered towards more randomized configurations, adds to our understanding of network-level neuropathology in SAD.

Keywords

graph theory; gray matter connectome; multivariate morphometry; social anxiety disorder; structural covariance network; support vector machine

1. Introduction

Social anxiety disorder (SAD) is a disabling psychiatric condition characterized by disproportionate fear or anxiety about social situations in which the individual is exposed to possible scrutiny (Dai *et al.*, 2017). It leads to various emotional, cognitive, and behavioural impairments (Ruscio *et al.*, 2008). Its high lifetime prevalence (7-12%) (Stein and Stein, 2008), high comorbidity with psychopathology (Meier *et al.*, 2015), typically chronic course and suboptimal therapeutic options (Penninx *et al.*, 2021) have motivated research into its neurobiological substrates, for which the non-invasive methods of magnetic resonance imaging (MRI) are particularly useful (Bas-Hoogendam *et al.*, 2022). The most consistent MRI findings in SAD are functional and/or structural abnormalities in cortical regions, notably prefrontal cortex (PFC), anterior cingulate cortex (ACC), insula, medial parietal and occipital regions, and in subcortical regions especially amygdala and putamen (the 'fear circuitry) (Bas-Hoogendam and Westenberg, 2020, Bruhl *et al.*, 2014a, Etkin and Wager, 2007, Groenewold *et al.*, 2023, Mizzi *et al.*, 2022, Zhang *et al.*, 2022b). This extends the classical neurofunctional model of SAD, highlighting the crucial roles of both dysfunctional bottom-up response and top-down regulation in its emotional, cognitive, and behavioural disabilities (Bas-Hoogendam and Westenberg, 2020, Bruhl *et al.*, 2014a, Etkin, 2012, Gentili *et al.*, 2016).

To date, MRI-based studies seeking to identify neuroimaging biomarkers for SAD have mainly focused on regional brain abnormalities in e.g. gray matter volume

(GMV), cortical thickness (CT), and local brain activity. However, the brain is increasingly seen as a system of interacting information-sharing networks (Damoiseaux *et al.*, 2006). Comprehensive characterization from a network perspective can deepen understanding of the structural and functional architecture of the whole brain (Sporns *et al.*, 2005), and may offer further insights into the neuropathology of psychiatric disorders as network-level disruptions rather than abnormalities in isolated brain areas (Zugman *et al.*, 2021). This analytical framework can be applied to several kinds of imaging data. Graph theoretical analyses based on gray matter (GM) functional connectivity and white matter (WM) structural connectivity have been widely used to characterize the abnormal brain connectome in psychiatric disorders (Crossley *et al.*, 2017, Yang *et al.*, 2021), but both approaches have some technical issues: functional connectivity measured using blood oxygen level-dependent (BOLD) MRI is vulnerable to the variability of brain states (Finn *et al.*, 2017), and reconstruction of WM structural connectivity is restricted by tractography algorithms (Girard *et al.*, 2014). A more recent third application, offering complementary insights, is to GM morphological covariance systems, which yield relatively stable neurobiological phenotypes based on the anatomical organization of large-scale brain networks (Alexander-Bloch *et al.*, 2013a, Evans, 2013, He *et al.*, 2007, Liu *et al.*, 2021, Seidlitz *et al.*, 2018). To understand what GM covariance means, we must understand its origin and cause. At one level of explanation, morphological covariance arises from both GM functional connections and WM structural connectivities: synchronous activities and/or direct connections prompt

neuronal synaptogenesis that results in mutual neurotrophic reinforcement between brain regions, promoting coordinated regional development or maturation (Alexander-Bloch *et al.*, 2013a, Alexander-Bloch *et al.*, 2013b, Evans, 2013, Seidlitz *et al.*, 2018). This anatomical/functional relationship is manifest in the substantial overlap between GM morphological covariance and GM functional or WM connections (Alexander-Bloch *et al.*, 2013b, Gong *et al.*, 2012). At another level of explanation, patterns of structural covariance reflect the influences of genetic pleiotropy, environmental influences, experience-related plasticity, neurodevelopment and ageing, and neuropathology (Alexander-Bloch *et al.*, 2013a, Evans, 2013, He *et al.*, 2007, Montembeault *et al.*, 2012). In psychiatric disorders there is increasing evidence of abnormalities of large-scale structural covariance networks (SCNs), partially corresponding to GM functional or WM structural network disruptions (Bassett *et al.*, 2008, Sharda *et al.*, 2016, Yun *et al.*, 2020). However, more work is needed to define the neurobiological significance of the SCNs. Here we attempt this for the GM morphological network in SAD.

Notwithstanding their great potential, identifying SCN-based biomarkers poses technical problems. First, many studies have use seed-based (rather than whole-brain) analyses to characterize specific networks (Qiu *et al.*, 2014). Second, SCNs are usually investigated by constructing a single brain network for each group, which makes it hard to characterise individual networks and relate them to clinical features (Alexander-Bloch *et al.*, 2013a). These considerations prompted development of a method combining probability density estimation and Kullback–Leibler

divergence-based similarity (KLS) to capture whole-brain interregional covariance for single-subject-level networks (Kong *et al.*, 2015, Kong *et al.*, 2014, Wang *et al.*, 2016), and this is increasingly used in the search for neuroimaging biomarkers for psychiatric disorders (Homan *et al.*, 2019, Lai *et al.*, 2022, Lei *et al.*, 2021). The third point concerns the choice of morphological metric. Many studies use regional GMV to construct SCNs; however GMV is a complex metric, mathematically the product of CT and cortical surface area (CSA), and with a complicated relationship to the 3D folding structure of the cortex. Another approach divides the GM into voxel cubes which reflects the local thickness and the 3D folding structure of the cortex (Tijms *et al.*, 2012); however, these cubes do not necessarily correspond to functionally or anatomically homogeneous regions (Kong *et al.*, 2014). Neither of these approaches takes full account of the complexity of cortical structure: the shape and size of a particular region often exhibits very high inter-person variability (Kong *et al.*, 2014). Moreover, given the distinct developmental trajectories and cytological and genetic differences of independent cortical structural metrics such as CT, CSA, and curvature (Ducharme *et al.*, 2015, Tamnes *et al.*, 2017), valuable information may be lost if they are compounded into a complex metric like GMV.

We therefore set out to use the KLS approach to characterize the topological organization of single-subject GM covariance networks in a relatively large and homogenous sample of SAD patients. We constructed networks based on four distinct morphological parameters: for cortical surface-based morphometry (SBM) we used two basic surface parameters, CT and CSA, to which we added a third metric

(curvature) representing the spatial complexity of cortex; for subcortical structures, known to be important in SAD (Bas-Hoogendam *et al.*, 2017, Bas-Hoogendam and Westenberg, 2020, Groenewold *et al.*, 2023, Zhang *et al.*, 2022b), we used volume-based morphometry (VMB) based on GMV. In addition, exploration analyses were conducted to explore the correlations of SCN abnormalities to clinical characteristics. Lastly, we used machine learning to investigate their potential diagnostic efficacy. In view of the paucity of evidence on GM covariance network in SAD and the exploratory nature of the our analyses, we did not set out to test specific hypotheses.

2. Materials and Methods

2.1. Subjects

In line with the ethical standards of the relevant national and institutional committees on human experimentation and with the Helsinki Declaration of 1975, as revised in 2008, this study was approved by the Medical Research Ethics Committee of West China Hospital of Sichuan University. All participants gave prior written informed consent. For the SAD group, 49 right-handed adult patients with SAD were recruited at the Mental Health Center of the West China Hospital of Sichuan University. According to the Diagnostic and Statistical Manual of Mental Disorders, Fourth Edition (DSM-IV), two experienced clinical psychiatrists established the diagnosis of SAD using the Structured Clinical Interview for DSM Disorders (SCID). Power

analysis using G Power software (Faul *et al.*, 2007) suggested that at least 102 subjects were required to obtain a medium-sized effect with adequate statistical power (Cohen's d = 0.5, $\alpha = 0.05$, $1-\beta = 0.8$ for an independent-sample t-test). For the healthy controls (HC) group, we recruited 53 demographically matched (i.e. sex, age, and handedness) individuals from the local community, in whom the SCID-Non-Patient Version confirmed lifetime absence of neurological and psychiatric disorders. The following exclusion criteria applied to all subjects: comorbidity with other axis I psychiatric disorders, axis II antisocial, or borderline personality disorders; current psychopharmacological/psychological therapy; history of substance dependence or abuse; learning or developmental disorders; history of head injury; presence of major neurological or physical diseases; family history of mental disorders; and current pregnancy, claustrophobia, or other contraindications to MRI examination.

Illness duration was defined as the period between the first reported or observed alterations in psychological or behaviour state and the moment of study participation (Singh et al., 2005), using information from patients, family members, and medical records. Symptom severity (i.e. social anxiety level) was assessed with the self-reported Liebowitz Social Anxiety Scale (LSAS) (Mennin *et al.*, 2002); the 24-item LSAS provides scores for fear factor (LSASF) and social avoidance factor (LSASA), their sum being the total score (LSAST). LSAS has shown good validity and reliability in Chinese populations (He and Zhang, 2004, Zhang *et al.*, 2020, Zhang *et al.*, 2022b).

2.2. Image acquisition and pre-processing

***Image acquisition*.** This study uses an SAD dataset in which we acquired, in a single session, whole-brain high-resolution three-dimensional T1-weighted images, resting-state functional MRI and diffusion tensor imaging data on a 3.0 T MR system (Siemens Trio, Erlangen, Germany) with a 12-channel head coil. During the scans subjects were asked to keep still, with closed eyes, relaxed but awake, and not think of anything deliberately. Earplugs were used to reduce scanner noise, and foam pads to minimize head motion. The high-resolution T1-weighted images used in this study were acquired using a spoiled gradient-recalled sequence with these parameters: inversion time 900 ms; repetition time 1900 ms; echo time 2.26 ms; flip angle 9°; 176 sagittal slices; slice thickness 1 mm; field of view 256 × 256 mm^2; data matrix 256 × 256; voxel size 1 × 1 × 1 mm^3. All scans were inspected by an experienced neuroradiologist to rule out visible artefacts and structural abnormalities.

Image pre-processing. Cortical SBM reconstruction and estimation of CT, CSA, and curvature were performed using the FreeSurfer package 7.2 (http://surfer.nmr.mgh.harvard.edu) with a 'recon-all' pipeline, described in detail elsewhere (Dale *et al.*, 1999, Fischl and Dale, 2000b, Fischl *et al.*, 1999). Briefly, the automatic process included motion correction, skull stripping using a deformable template model, automated registration to Talairach space, segmentation of subcortical WM and deep GM volumetric structures, intensity normalization, tessellation of GM and WM boundaries, automated topology correction and surface deformation following intensity gradients, surface inflation and registration to a

spherical atlas, and cortical parcellation (Desikan *et al.*, 2006, Fischl *et al.*, 2004). CT was defined as the average shortest distance between the WM/GM boundary and GM/cerebrospinal fluid boundary at each point (Fischl and Dale, 2000a), the CSA of each parcellation as the sum of the area of all tessellations on the surface (Palaniyappan *et al.*, 2011), and the curvature as the reciprocal of the radius of an inscribed circle (Cole *et al.*, 2014). For quality control, all reconstructed cortical surfaces were visually inspected by two experienced researchers blinded to participant information: when inaccuracies (e.g. skull strip failures, pial surface misplacement, segmentation errors, intensity normalization errors, topological defects) were identified, the images were manually edited (e.g. erasing/filling/cloning voxels, adding control points, etc) and re-analyzed (Fischl *et al.*, 2002, Reuter *et al.*, 2012); 8 subjects (7 SAD, 1 HC) were excluded from subsequent analyses due to failure to fix inaccurate reconstruction.

VBM reconstruction and GMV estimation were conducted using Statistical Parametric Mapping software (SPM12; Welcome Department of Cognitive Neurology, London, UK; http://www.fil.ion.ucl.ac.uk/spm/) (Ashburner and Friston, 2005). After manual reorientation to the anterior commissure, images were segmented into GM, WM and cerebrospinal fluid with the new segmentation tool; the GM data were aligned, resampled to $2\times2\times2$ mm^3, and normalized to Montreal Neurological Institute (MNI) space using Diffeomorphic Anatomical Registration Through Exponential Lie Algebra (DARTEL), modulated for preservation of GMV (through multiplying by the Jacobian determinants derived from the normalization), then smoothed with an 8 mm

full-width at half-maximum Gaussian kernel (Ashburner, 2007). This yields the GMV maps with morphological intensity information of each voxel for each participant, of which two experienced researchers independently checked the quality. For comparability, the 8 subjects excluded from the SBM analyses were also excluded from further VBM analyses.

2.3. Structural covariance network construction

Network construction. We constructed single-subject SCNs using an approach that quantifies inter-regional relations by determining the similarity of estimated probability distributions of morphological metrics for pair-wise brain regions (Kong *et al.*, 2015, Kong *et al.*, 2014). We used the Desikan-Killiany atlas (Desikan *et al.*, 2006) for SBM and the Automated Anatomical Labeling (AAL) atlas (Tzourio-Mazoyer *et al.*, 2002) for VBM to parcellate whole brain GM into 68 and 90 regions of interest (ROIs), respectively: these are the network nodes (Figure 1A). For each subject, the probability density function (PDF) of the regional morphometry (i.e. CT, CSA, curvature, and GMV for each ROI) was calculated (Botev *et al.*, 2010) using a kernel density estimator toolbox in MATLAB[1] which employs a Gaussian kernel by default and automatically selects the optimal bandwidth (Botev *et al.*, 2010). Next, Kullback–Leibler (KL) divergence was calculated between the PDFs of pair-wise ROIs as a measure of statistical similarity (Figure 1B) (Van Erven and Harrëmos, 2014): these are the network edges. KL divergence evaluates

[1] https://www.mathworks.com/matlabcentral/ fileexchange/14034-kernel-density-estimator

similarity/dissimilarity of one probability distribution (say p) to another (q) (Van Erven and Harrëmos, 2014), which is calculated as follows:

$$\mathrm{KL}(p\|q) = \sum_{i=1}^{n}\left(p(i)\log\frac{p(i)}{q(i)}\right)$$

As the effect of n (the number of sample points) on PDF estimation is a decreasing function (Wang *et al.*, 2016), we used a conservative value of n = 512 (Homan *et al.*, 2019). Because KL (p||q) does not equal KL (q||p), we assessed the similarity between the two PDFs using a symmetric KL divergence (KL(p, q)) (Homan *et al.*, 2019, Kong *et al.*, 2015, Kong *et al.*, 2014, Wang *et al.*, 2016), calculated as:

$$\mathrm{KL}(p,q) = \sum_{i=1}^{n}\left(p(i)\log\frac{p(i)}{q(i)} + q(i)\log\frac{q(i)}{p(i)}\right)$$

Finally, the value of symmetric KL divergence was converted to a similarity measurement (range 0 [no similarity] to 1 [identical distributions]) for all pair-wise regions (Homan *et al.*, 2019, Kong *et al.*, 2015, Kong *et al.*, 2014, Wang *et al.*, 2016):

$$\mathrm{KLS}(p,q) = e^{-KL(p,q)}$$

For each subject, this yields four KLS-based SCNs: three 68 × 68 matrixes based on CT, CSA, and curvature, and a 90 × 90 matrix based on GMV (Figure 1C).

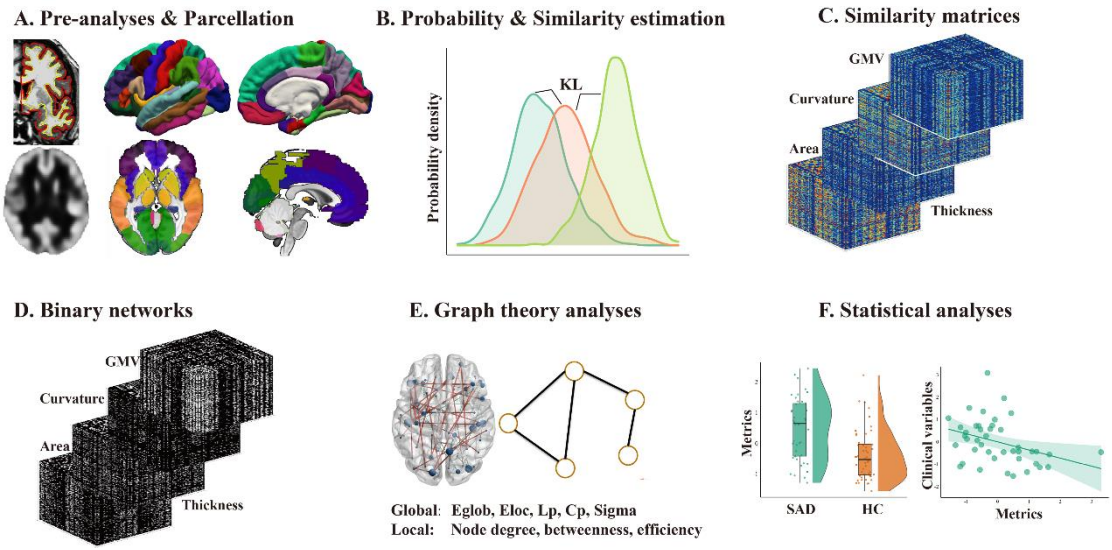

Figure 1. The analysis of structural covariance networks. (A) Cortical reconstruction and estimation of CT, CSA, and curvature were performed using FreeSurfer, and GMV estimated using Statistical Parametric Mapping. Whole brain GM was parcellated using the Desikan-Killiany atlas for cortical morphometry (CT, CSA, curvature: 68 regions) and the AAL atlas for GMV (90 regions). (B) The PDF of each regional morphometry (CT, CSA, curvature, GMV) was calculated using kernel density estimation, and KL divergence measured statistical similarity between the PDFs of pair-wise regions. (C) For each subject, the structural covariance network is represented by the resulting cortical morphometry (68×68) and GMV (90×90) matrix. (D) These were binarized over a wide range of sparsity S thresholds. (E) For each subject, global and nodal metrics characterize the topological properties of these binarized structural covariance networks. (F) The network metrics were compared between SAD and HC using independent-sample t test, and those showing significant between-group differences were analysed by partial correlation to investigate the association with clinical features. Abbreviations: AAL, Automated Anatomical Labeling; C_p, clustering coefficient; E_{glob}, global efficiency; E_{loc}, local efficiency; HC, healthy controls; KL, Kullback-Leibler; L_p, characteristic path length; PDF, probability density function; SAD, social anxiety disorder.

Network binarization. Topological graph-theoretical analysis requires all the subjects' networks to have the same number of nodes and edges, so we applied a wide range of sparsity S (i.e. the number of actual edges as a fraction of all possible edges) thresholds (0.05-0.30 with an interval of 0.01) to binarize the KLS-based matrices (Lai *et al.*, 2022) (Figure 1D): in these binarized SCNs, 1 denotes significant covariation of pair-wise areas, while 0 represents none. All these procedures were completed in MATLAB R2014a (The MathWorks, Inc., MA, USA).

2.4. Graph theoretical analysis

***Topological property calculation*.** We used the Brain Connectivity Toolbox (https://sites.google.com/site/bctnet/Home; (Rubinov and Sporns, 2010)) in MATLAB R2014a to quantify the topological properties of the binarized SCNs, calculating all parameters at each sparsity threshold (Figure 1E). Details of these topological parameters are given elsewhere (Rubinov and Sporns, 2010; Latora and Marchiori, 2001, Watts and Strogatz, 1998); here we summarise the main points. Network parameters are quantified at both the global and nodal levels.

The global-level parameters comprise the small-world metrics and the network efficiency parameters. First, the global small-world metrics: the *clustering coefficient* (Cp) reflects the local 'cliquishness' of a node in a network (i.e. the fraction of a node's neighboring nodes which are interconnected) and the C_p of the network is the average of C_p over all nodes; the *characteristic path length* (L_p) is the mean shortest distance between pairs of nodes, calculated by averaging the smallest number of

connections required to link any pair of nodes; and the *small-worldness* (σ) quantifies the small-world topology, calculated as normalized C_p divided by normalized L_p. To assess small-worldness, the C_p and L_p of the networks were compared with those ($C_{prandom}$ and $L_{prandom}$) of random networks (n = 100) that preserved the same number of nodes and edges, and the same degree distribution, as the real brain networks (Maslov and Sneppen, 2002, Wang *et al.*, 2015). Typically, a small-world network meets the conditions of normalized $C_p = C_p/C_{prandom} > 1$ and normalized $L_p = L_p/L_{prandom} \approx 1$; thus the small-world scalar $\sigma > 1$ (Watts and Strogatz, 1998). Next, the global network efficiency metrics: the *global efficiency* (E_{glob}) measures the global efficiency of parallel information transfer; the *local efficiency* (E_{loc}) measures local connectedness (i.e. the communication efficiency among the immediate neighbors of a node when it is removed). In addition to these global parameters, there are three nodal-level centrality parameters: *nodal degree* is the number of nodes directly connected to a particular node; *betweenness* measures the number of shortest paths between all other pairs of nodes through this node; and *nodal efficiency* refers to the information transmission capability of each node in the network.

Area under the curve computation. As sparsity threshold affects network small-worldness (He *et al.*, 2008), we calculated the area under the curve (AUC) over a range of sparsity thresholds (0.05-0.30 with an interval of 0.01), as a comprehensive scalar measure of brain network topology, which avoids potential bias of any single threshold.

2.5. Network-based statistical analyses

Group comparison of network metrics. The AUC of network metrics were compared between SAD and HC using independent-sample t test with age, sex, and total intracranial volume (TIV) as covariates of no interest. For any all SCNs, when comparing graph theoretical metrics between two groups we applied the Benjamin–Hochberg False Discovery Rate (FDR) to correct for multiple comparisons with a significance level of $P < 0.05$ (Genovese *et al.*, 2002).

Clinical relevance analyses. To identify relationships in the SAD cohort between the network properties with significant between-group differences and clinical characteristics (LSASA, LSASF, and disease duration), partial correlation analyses were conducted with age, sex, and TIV as covariates. FDR was used to control for multiple comparisons with $P < 0.05$.

Machine learning analyses. Support vector machine (SVM) analyses (Cortes and Vapnik, 1995), using the LIBSVM toolbox (Chang and Lin, 2011), explored how well the graph-theoretical matrices could discriminate SAD versus HC at the individual level. In brief, we vectorised the graph-theoretical matrices showing significant between-group differences for each subject as features for subsequent analyses; leave-one-out cross-validation was used to separate training and testing sets; data normalization on the feature matrix and optimization of the SVM hyperparameter (the soft margin parameter C) on the training sets were performed in each iteration; the SVM classification algorithm with linear kernel was used to find the hyperplane

maximizing the separation margin between binary classes in the feature space within a training set; this classification strategy was then used to predict the class of the testing sets; classification performance of the model was evaluated on the testing sets through sensitivity, specificity, total accuracy, and the area under the receiver operating characteristic (ROC) curve (AUC); a nonparametric permutation test (5000 times) was conducted to estimate significance for the machine learning model. More details see *Supplementary Materials*.

3. Results

3.1. Demographic and clinical characteristics

There were no significant differences between SAD and HC in sex composition and age; SAD patients scored significantly higher on LSAS (Table 1).

Table 1. Demographic and clinical characteristics of participants

Characteristics	**SAD (N = 42)**	**HC (N = 52)**	***P* value**
Sex (Male/Female)	25/17	31/21	0.993[a]
Age (years)	24.2 ± 5.5	23.4 ± 3.4	0.387[b]
Illness duration (years)	6.9 ± 4.1	-	-
LSAST	64.3 ± 24.1	18.3 ± 8.3	< 0.001[b]
LSASF	31.7 ± 11.8	10.1 ± 5.4	< 0.001[b]
LSASA	32.6 ± 13.4	8.2 ± 6.0	< 0.001[b]

Note: Continuous variables are presented as the means ± standard deviations. [a] by chi-square test. [b] by independent-sample t test. Abbreviations: HC, healthy controls; LSAST, LSASF, and LSASA, total score and fear and avoidance factor scores on the Liebowitz Social Anxiety Scale (LSAS); SAD, social anxiety disorder.

3.2. Group differences in topological metrics of SCNs

Of the global topological characteristics, the curvature-based SCNs showed significant between-group differences: compared to HC, SAD patients showed significantly higher E_{glob} ($t = 3.473$, $P < 0.001$), shorter L_p ($t = -3.576$, $P < 0.001$), and stronger σ ($t = 2.258$, $P = 0.026$) (Figure 2). No significant global-level topological results were observed in the SCNs based on CT, CSA, or GMV.

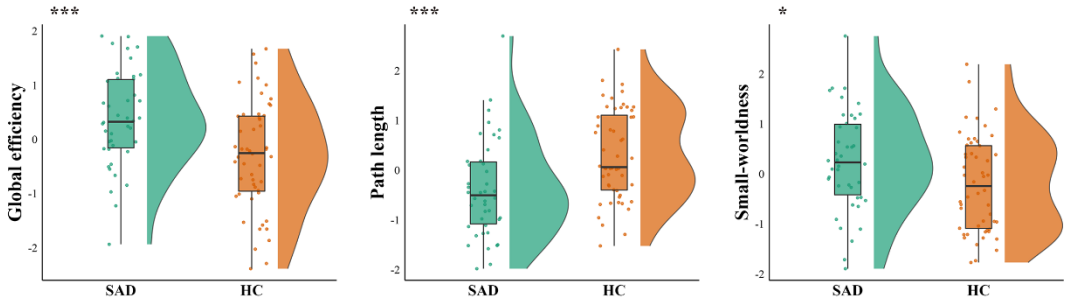

Figure 2. Intergroup comparisons between SAD patients and HC of global metrics for curvature-based structural covariance networks. Results for each metric are shown as a box plot with individual data points and a smoothed distribution; scores on the y-axis represent the standardized residuals of the graph-theoretical metrics after controlling for age, sex and total intracranial volume (*$P < 0.05$, ***$P < 0.001$). Abbreviations: HC, healthy controls; SAD, social anxiety disorder.

Of the nodal topological characteristics, in the SBM-based covariance network,

SAD patients showed increased nodal degree and efficiency in left superior frontal gyrus (SFG), right lingual gyrus (LG), and right superior parietal lobe (SPL), increased nodal efficiency in right pericalcarine cortex, and decreased nodal degree in right paracentral gyrus; in the VBM-based covariance network, SAD showed increased nodal degree in left amygdala (Figure 3 and Table S1).

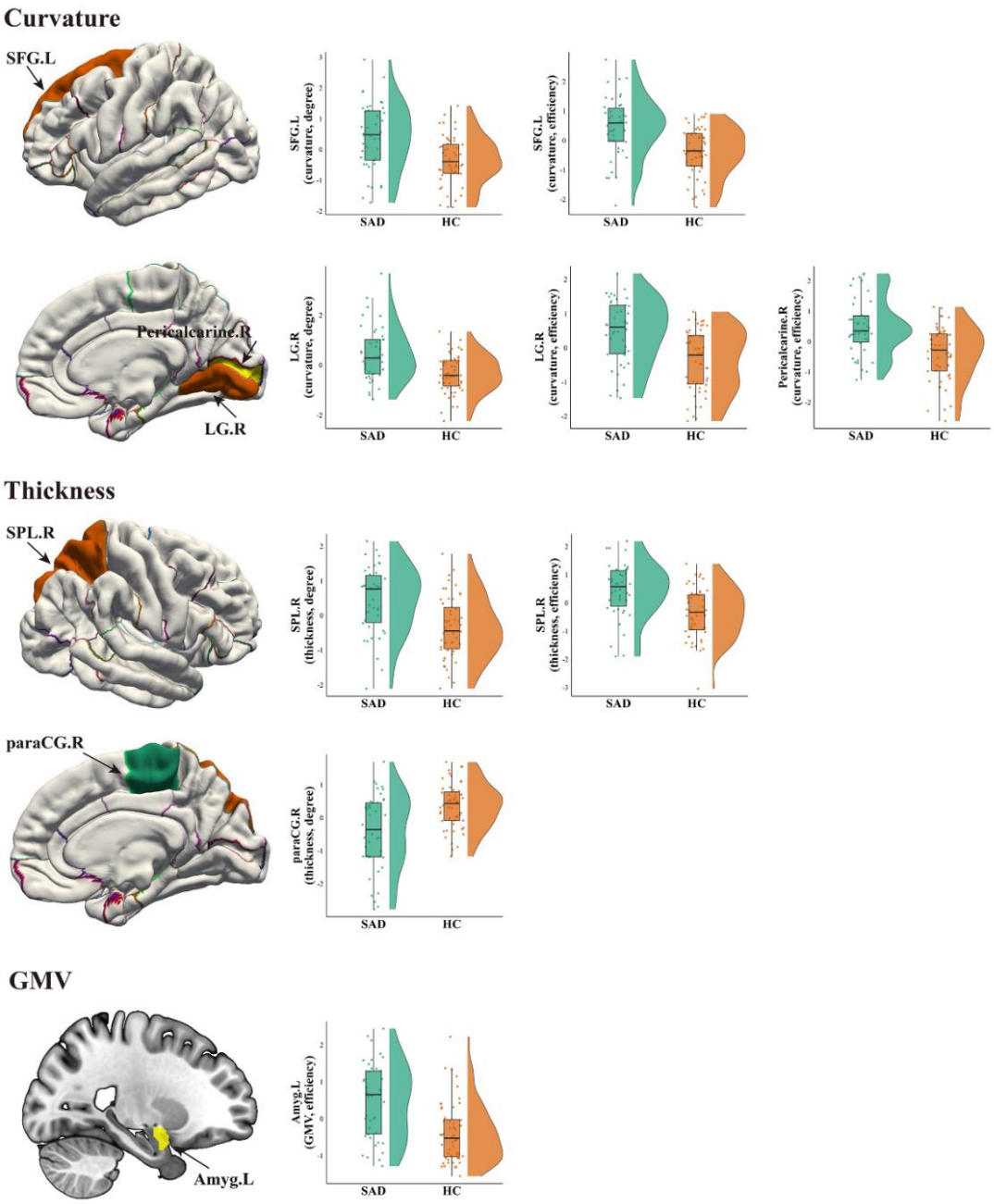

Figure 3. Intergroup comparisons between SAD patients and HC of nodal centrality for structural covariance networks. Results for each metric are shown as a box plot with individual data points and a smoothed distribution; the y-axis represents the standardized residuals of the nodal centrality metrics after controlling for age, sex and total intracranial volume; the brain image shows the anatomical location. Abbreviations: GMV, gray matter volume; HC, healthy controls; L, left; LG, lingual gyrus; paraCG paracentral gyrus; R, right; SAD, social anxiety disorder; SFG, superior frontal gyrus; SPL, superior parietal lobe.

3.3. Clinical correlates of network topological characteristics

After controlling for the confounders of sex, age and TIV, at the global level of the curvature covariance network, E_{glob} (r = 0.424, P = 0.007) and σ (r = 0.480, P = 0.002) were positively correlated to illness duration, while L_p was negatively correlated with duration (r = -0.415, P = 0.009) (Figure 4). At the nodal level, there were significant positive correlations between curvature-based nodal degree of right LG and LSASA (r = 0.386, P = 0.015), between curvature-based nodal efficiency of right LG and LSASA (r = 0.342, P = 0.033); and between curvature-based nodal efficiency of right pericalcarine cortex and illness duration (r = 0.470, P = 0.003). Only the correlation between σ of curvature covariance network and duration survived correction for multiple tests at FDR-corrected $P < 0.05$.

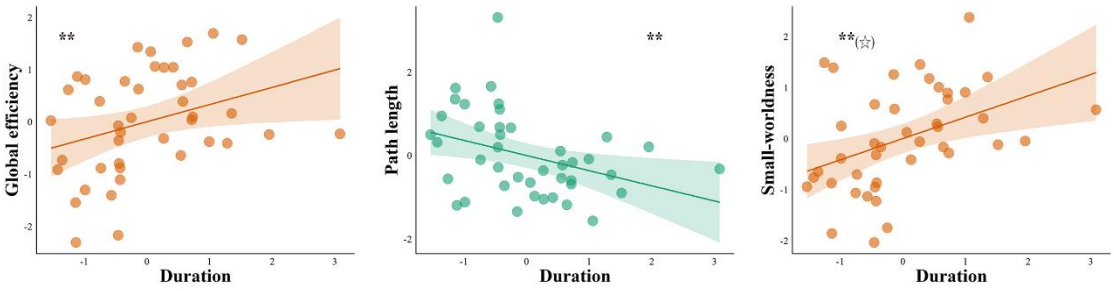

Figure 4. Clinical correlates of global metrics for curvature-based structural covariance networks. Scatter plots depicting the relationship between illness duration and global-level graph-theoretical metrics with significant between-group differences in social anxiety disorder patients (**$P < 0.01$). The x-axis represents the standardized residuals of the illness duration, the y-axis the standardized residuals of the graph-theoretical metrics, after sex, age, and total intracranial volume were regressed out. Only for the small-worldness of the curvature covariance network (right-hand panel) did the correlation with duration survive correction for multiple tests at FDR-corrected $P < 0.05$.

3.4. Single-subject classification of SAD patients versus HC

The accuracy of SVM classification for SAD versus HC based on the significantly-different network topological characteristics were significantly above chance ($P < 0.001$), with total accuracy 78.7%, sensitivity 83.3%, specificity 80.8%, and AUC 86.8% (Figure 5).

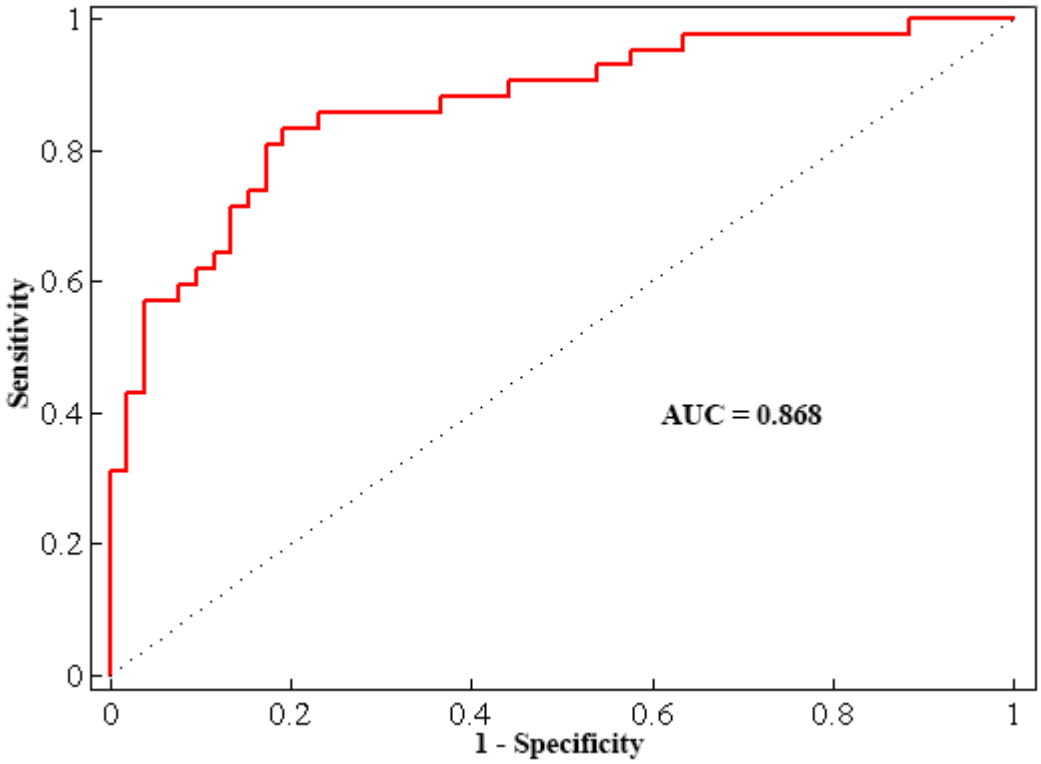

Figure 5. Single-subject classification of SAD patients versus HC based on the significant network topological characteristics. Abbreviations: AUC, area under the receiver operating characteristic curve; HC, healthy controls; SAD, social anxiety disorder.

4. Discussion

We believe this is the first study to characterise brain single-subject GM connectome disorganization based on comprehensive structural metrics (CT, CSA, curvature, and GMV) in a relatively large and homogeneous sample of SAD patients. SAD patients showed greater network integration, reflected by higher E_{glob}, shorter L_p, and stronger σ of curvature-based SCNs, and altered nodal centralities in the cognitive-control/emotional regulation systems (SFG, SPL, amygdala) and sensorimotor/perceptual systems (paracentral gyrus, LG, pericalcarine cortex). Altered

global and nodal topological metrics correlated with symptom severity and illness duration, suggesting pathophysiological relevance. Further, graph-based metrics allowed single-subject classification of SAD versus HC with significant accuracy, suggesting potential diagnostic efficacy. These findings offer some insights into the neural substrates of SAD, as we now discuss.

In formal terms, the normal human brain is configured as a small-world network that optimally balances local segregation (reflected by C_p and E_{loc}) and global integration (reflected by L_p and E_{glob}) to maximize efficient information processing at low wiring and energy costs (Bullmore and Sporns, 2012, Sporns and Zwi, 2004). In contrast, a regular network is characterized by high segregation and low integration, while a random network demonstrates high integration and low segregation (Suo et al., 2018). Consequently, our findings in single-subject GM SCNs of higher structural network integration (i.e. higher Eglob, shorter Lp, and stronger σ) and relative preservation of segregation in SAD patients suggest a shift toward more randomized configurations. This is consistent with reports of globally disrupted topology in GM functional networks (SAD patients having shorter normalized Lp than HC) (Yang *et al.*, 2019). Indeed, a shift toward more randomized global network topology is reported in many psychiatric disorders (Lei et al., 2022, Niu et al., 2018, Singh et al., 2013). Compared with the small-world model, randomized networks show less modularized information processing and fault tolerance (Latora and Marchiori, 2001), as well as aberrant signal propagation speed and synchronizability (Strogatz, 2001). Although the neurobiological mechanisms remains to be established, a shift toward

randomization may underpin deficient transmission of information and thus contribute to cognitive, emotional, and behavioral impairments in SAD (Latora and Marchiori, 2001). Such a pathophysiological link is supported by the correlation between relative randomized organization and SAD duration: the longer the disease, the more prominent the shift to a random pattern (Liao *et al.*, 2017).

At a regional level, higher nodal centralities, suggesting important roles in the network (Liao *et al.*, 2017), were observed in left SFG, right SPL, and left amygdala, which are core regions involved in cognitive control and emotional regulation (Bruhl *et al.*, 2014a). This is in line with reported regional structural and functional abnormalities in SAD (Bruhl *et al.*, 2014a, Bruhl *et al.*, 2014b, Mizzi *et al.*, 2022, Zhang *et al.*, 2020); a recent systematic review of SAD most consistently implicated resting-state dysconnectivity in PFC, parietal lobe, and amygdala (Mizzi *et al.*, 2022). As a key node of the frontolimbic circuitry (fear circuitry), PFC plays a central role in cognitive control and emotional regulation such as appraisal and reappraisal, self-referential judgments, attentional allocation towards emotional stimuli, inhibition and memory extinction of fear and anxiety responses (Etkin *et al.*, 2011, Hiser and Koenigs, 2018, Raichle, 2015, Zhang *et al.*, 2022a); the amygdala is implicated in detecting and evaluating environmental cues, arousal and negative valence, acquisition, consolidation and retrieval of fear memory, as well as extinction of fear (Janak and Tye, 2015, Sergerie *et al.*, 2008). It is accepted that inhibition by PFC of activity in limbic regions such as amygdala is vital for well-balanced fear responses, without which unchecked amygdala activity maintains the learned aversive response

in the presence of SAD-related stimuli (Davidson, 2002, Marek *et al.*, 2013). Disturbed and dysregulated attentional networks in the frontoparietal circuits (dorsolateral PFC, SPL) are also thought to be associated with the abnormalities that characterize SAD in executive function, attentional allocation (top-down management of rules and goals during externally directed tasks (Turner and Spreng, 2012)), and emotional regulation (Ochsner *et al.*, 2012, Sylvester *et al.*, 2012). Our findings of abnormal nodal centralities in PFC, SPL, and amygdala may underlie these neural mechanisms of hypervigilance and persistent biased attentiveness to potential social threatening stimuli, deficient cognitive control, and dysfunctional emotional regulation (Bruhl *et al.*, 2014a, Sylvester *et al.*, 2012).

We also observed altered nodal centralities in the right paracentral gyrus, LG, and pericalcarine cortex, which comprise the sensorimotor network (SMN) and visual network (VN) (Bruhl *et al.*, 2014a), in both of which structural/functional abnormalities have been reported in SAD (Chavanne and Robinson, 2021, Dixon *et al.*, 2020, Goldin *et al.*, 2009, Talati *et al.*, 2013). There is increasing evidence that the perceptual/sensorimotor system is involved in emotion perception and experience (Hardee *et al.*, 2017), perception of social facial signals of fear (Pourtois *et al.*, 2004), and emotion regulation in responses to SA-related cues (Kropf *et al.*, 2019). Disrupted processing of sensorimotor/visual signals, perceptual impairments, and dysfunctional cognitive control in the high-order networks, may all contribute to inappropriate processing of external social signal, abnormal emotional arousal, and resultant cognitive bias and avoidance behaviour (Kreifelts *et al.*, 2019, Kreifelts *et al.*, 2020).

Intriguingly, the SCNs constructed from different morphological indices revealed different alterations of network topology. In a sense, those results were consistent with extant evidence of the metric specificity of the topological organization of morphological similarity networks in physiological and pathological conditions (He *et al.*, 2008, Sanabria-Diaz *et al.*, 2010). In technical terms, SCNs constructed by different surface morphological metrics have different interregional covariance and network topology (Li *et al.*, 2021). Biologically, these likely reflect morphological architectures with different developmental trajectory, cytology, and genetics (Chen *et al.*, 2013, Hogstrom *et al.*, 2013, Rakic, 1988, Storsve *et al.*, 2014, Tamnes *et al.*, 2017), whereas developmental, genetic pleiotropy, and environmental factors may influence the structural covariance among brain regions, thus producing unique structural covariance patterns of individuals (Alexander-Bloch *et al.*, 2013a, Evans, 2013, He *et al.*, 2007). One plausible explanation, therefore, for the discrepancies between different morphological networks in SAD patients is that they reflect these differences in the particular developmental, genetic and environmental contexts (Li *et al.*, 2021). Direct empirical studies (e.g., cytoarchitectonic) studies are warranted to investigate this further.

We present here the first preliminary evidence that graph-theoretical topological matrices of SCNs allow individual classification of SAD versus HC. Neuroimaging analyses combined with machine learning offer the hope of developing objective biomarkers (Chen *et al.*, 2020, Frick *et al.*, 2014, Liu *et al.*, 2015, Zhan *et al.*, 2021) to guide early diagnosis and timely interventions in clinical practice (Bas-Hoogendam

and Westenberg, 2020, Etkin, 2019). It is however a long road to clinical application in psychiatry. Published machine learning pipelines differ in technical aspects (feature selection and extraction, classification models, validation methods, performance evaluations), and sample sizes in research studies are usually relatively small. Practical factors (e.g. clinical heterogeneity, availability and comparability of neuroimaging data acquisition, cost) have limited the application of neuroimaging metrics in classifying or stratifying individual patients (Bondi *et al.*, 2023, Rashid and Calhoun, 2020). At this stage, machine learning analyses may be more informative in exploring the distinct patterns of SCNs constructed by different morphological indices in psychiatric disorders, with a view to gaining insights into their neurobiology.

This study has limitations. First, no cross-sectional design can identify causal associations between SCNs abnormalities and disease: this will need longitudinal studies of subjects with high vulnerability to developing SAD (e.g. based on genotypes and endophenotypes (Bas-Hoogendam *et al.*, 2016)), and interventional (therapeutic) trials. Second, it would have been desirable to match the two groups for general cognitive ability: however, there is no definite evidence that SAD patients suffer from intellectual impairment (Stein and Stein, 2008), so we do not consider general cognitive ability a significant confounder. Third, to explore the specific neurobiological substrates of SAD, we recruited adult patients without any comorbid disorders; however, to establish whether these neurostructural alterations are specific for SAD, rather than trans-diagnostic features of psychiatric disorders, will require further trans-diagnostic studies, of particular importance for SAD given the high

psychopathological comorbidity (Meier *et al.*, 2015). Fourth, although we recruited enough participants to ensure adequate statistical power, the final sample size dropped due for image quality reasons, and is therefore not very large compared to recent studies exploring other psychiatric disorders. Fifth, there are no universally accepted methods to define network nodes and edges (de Reus and van den Heuvel, 2013). To facilitate comparison with the literature, we made the methodologically conservative choice of the most commonly-used surface atlas (Desikan-Killiany) and structural atlas in volume space (AAL) as parcellation schemes to define network nodes. Nevertheless, brain network properties are influenced by parcellation templates (Li *et al.*, 2021, Ren *et al.*, 2019, Wang *et al.*, 2016, Zalesky *et al.*, 2012), and no single method meets all the challenges (Arslan *et al.*, 2018). Consequently, our observations need to be validated across different parcellation approaches. Additionally, we adopted the Kullback–Leibler divergence-based similarity approach to define the network edges. This methodological choice can influence network characteristics and reliability (Li *et al.*, 2021, Sarwar *et al.*, 2019, Zalesky *et al.*, 2012), and so it would be useful to replicate our findings using other methods (e.g., Jensen-Shannon divergence-based similarity (Li *et al.*, 2021)) to estimate interregional connectivities. Sixth, opinion is divided on whether to conduct smoothing before SCN construction, and what the optimal smoothing kernel size is for different morphological metrics; referring to previous studies (Homan *et al.*, 2019, Lai *et al.*, 2022), we made the conservative chose not to perform smoothing, but exploration of different choices would be useful (Li *et al.*, 2021) . Seventh, machine learning in our study should be

seen as a validation of between-group differences of graph-theoretical matrices and a preliminary exploration of their potential diagnostic value: we could only use leave-one-out cross-validation due to limited sample size, and our classification accuracy estimates may be inflated because we selected the graph-theoretical matrices showing significant between-group differences as features for SVM analyses (Kriegeskorte *et al.*, 2009). Larger and independent samples are needed in future studies.

In conclusion, based on graph-theoretical analysis of the single-subject GM covariance connectome, this study identified in SAD patients a shift toward randomized configurations, a sub-optimal topological organization reflected by higher network integration, and aberrant nodal centralities involving cognitive-control and emotional-regulation networks and the sensorimotor/perceptual systems, some of which were correlated to symptom severity and disease duration. These aberrant GM topological metrics have some ability to discriminate SAD from HC at the individual level. This study extends previous understandings of the neuroanatomical substrates of SAD, and demonstrates the potential of graph-theoretical measures of the GM covariance connectome as imaging biomarkers for clinical diagnosis.

Funding

This study was supported by National Key R&D Program of China (2022YFC2009900) and the National Natural Science Foundation of China (Grant Nos. 81621003, 81761128023, 81820108018, 82027808). The funding sources had no involvement in the study design, data collection and analysis, results interpretation, or writing of the paper.

Acknowledgements

The authors would like to express their sincere appreciation to supervisor and colleagues for valuable advice. We also thank all the participants in this study.

Conflict of Interest disclosure

The authors declare no conflict of interest.

Author contributions

XZ and HL conceptualized and designed the study. QYG and SW supervised the conduct of the study. XZ, HL, QYL, XY, NFP, and MH contributed to the data collection. XZ and HL performed the data analysis, results interpretation, and visualization, original draft writing and editing. SW and GJK provided interpretive advice and critically revised the manuscript, which all authors reviewed and approved for publication.

Data availability statement

The data and code that support the findings of present study are available from the

corresponding author through reasonable request. The data and code sharing adopted by the authors comply with the requirements of the funding institute and with institutional ethics approval.

References

Alexander-Bloch A, Giedd JN & Bullmore E. 2013a. Imaging structural co-variance between human brain regions. *Nat Rev Neurosci*. 14:322-36.

Alexander-Bloch A, Raznahan A, Bullmore ET & Giedd J. 2013b. The Convergence of Maturational Change and Structural Covariance in Human Cortical Networks. *Journal of Neuroscience*. 33:2889-+.

Arslan S, Ktena SI, Makropoulos A, Robinson EC, Rueckert D & Parisot S. 2018. Human brain mapping: A systematic comparison of parcellation methods for the human cerebral cortex. *Neuroimage*. 170:5-30.

Ashburner J. 2007. A fast diffeomorphic image registration algorithm. *Neuroimage*. 38:95-113.

Ashburner J & Friston KJ. 2005. Unified segmentation. *Neuroimage*. 26:839-851.

Bas-Hoogendam JM, Blackford JU, Bruhl AB, Blair KS, van der Wee NJA & Westenberg PM. 2016. Neurobiological candidate endophenotypes of social anxiety disorder. *Neurosci Biobehav Rev*. 71:362-378.

Bas-Hoogendam JM, Groenewold NA, Aghajani M, Freitag GF, Harrewijn A, Hilbert K, Jahanshad N, Thomopoulos SI, Thompson PM, Veltman DJ, Winkler AM, Lueken U, Pine DS, van der Wee NJA, Stein DJ & Group EN-AW. 2022. ENIGMA-anxiety working group: Rationale for and organization of large-scale neuroimaging studies of anxiety disorders. *Hum Brain Mapp*. 43:83-112.

Bas-Hoogendam JM, van Steenbergen H, Pannekoek JN, Fouche JP, Lochner C, Hattingh CJ, Cremers HR, Furmark T, Mansson KNT, Frick A, Engman J, Boraxbekk CJ, Carlbring P, Andersson G, Fredrikson M, Straube T, Peterburs J, Klumpp H, Phanp KL, Roelofs K, Veltman DJ, van Tol MJ, Stein DJ & van der Wee NJA. 2017. Voxel-based morphometry multi-center mega-analysis of brain structure in social

anxiety disorder. *Neuroimage-Clinical*. 16:678-688.

Bas-Hoogendam JM & Westenberg PM. 2020. Imaging the socially-anxious brain: recent advances and future prospects. *F1000Res*. 9:

Bassett DS, Bullmore E, Verchinski BA, Mattay VS, Weinberger DR & Meyer-Lindenberg A. 2008. Hierarchical organization of human cortical networks in health and schizophrenia. *J Neurosci*. 28:9239-48.

Bondi E, Maggioni E, Brambilla P & Delvecchio G. 2023. A systematic review on the potential use of machine learning to classify major depressive disorder from healthy controls using resting state fMRI measures. *Neurosci Biobehav Rev*. 144:104972.

Botev ZI, Grotowski JF & Kroese DP. 2010. Kernel Density Estimation Via Diffusion. *Annals of Statistics*. 38:2916-2957.

Bruhl AB, Delsignore A, Komossa K & Weidt S. 2014a. Neuroimaging in social anxiety disorder-a meta-analytic review resulting in a new neurofunctional model. *Neurosci Biobehav Rev*. 47:260-80.

Bruhl AB, Hanggi J, Baur V, Rufer M, Delsignore A, Weidt S, Jancke L & Herwig U. 2014b. Increased cortical thickness in a frontoparietal network in social anxiety disorder. *Human Brain Mapping*. 35:2966-2977.

Bullmore E & Sporns O. 2012. The economy of brain network organization. *Nat Rev Neurosci*. 13:336-49.

Chang C-C & Lin C-J. 2011. LIBSVM: A library for support vector machines. *ACM Transactions on Intelligent Systems and Technology*. 2:1-27.

Chavanne AV & Robinson OJ. 2021. The Overlapping Neurobiology of Induced and Pathological Anxiety: A Meta-Analysis of Functional Neural Activation. *Am J Psychiatry*. 178:156-164.

Chen CH, Fiecas M, Gutierrez ED, Panizzon MS, Eyler LT, Vuoksimaa E, Thompson WK, Fennema-Notestine C, Hagler DJ, Jernigan TL, Neale MC, Franz CE, Lyons MJ, Fischl B, Tsuang MT, Dale AM & Kremen WS. 2013. Genetic topography of brain morphology. *Proceedings of the National Academy of Sciences of the United States of America*. 110:17089-17094.

Chen J, Zang Z, Braun U, Schwarz K, Harneit A, Kremer T, Ma R, Schweiger J, Moessnang C, Geiger L, Cao H, Degenhardt F, Nöthen MM, Tost H, Meyer-Lindenberg A & Schwarz E. 2020. Association of a Reproducible Epigenetic Risk Profile for Schizophrenia With Brain Methylation and Function. *JAMA Psychiatry*. 77:628-636.

Cole MW, Bassett DS, Power JD, Braver TS & Petersen SE. 2014. Intrinsic and task-evoked network architectures of the human brain. *Neuron*. 83:238-51.

Cortes C & Vapnik V. 1995. Support-vector networks. *Machine Learning*. 20:273-297.

Crossley NA, Marques TR, Taylor H, Chaddock C, Dell'Acqua F, Reinders AA, Mondelli V, DiForti M, Simmons A, David AS, Kapur S, Pariante CM, Murray RM & Dazzan P. 2017. Connectomic correlates of response to treatment in first-episode psychosis. *Brain*. 140:487-496.

Dai Q, Yang G, Hu C, Wang L, Liu K, Guang Y, Zhang R, Xu S, Liu B, Yang Y & Feng Z. 2017. The alienation of affection toward parents and influential factors in Chinese left-behind children. *Eur Psychiatry*. 39:114-122.

Dale AM, Fischl B & Sereno MI. 1999. Cortical surface-based analysis. I. Segmentation and surface reconstruction. *Neuroimage*. 9:179-94.

Damoiseaux JS, Rombouts SA, Barkhof F, Scheltens P, Stam CJ, Smith SM & Beckmann CF. 2006. Consistent resting-state networks across healthy subjects. *Proc Natl Acad Sci U S A*. 103:13848-53.

Davidson RJ. 2002. Anxiety and affective style: role of prefrontal cortex and amygdala. *Biol Psychiatry*. 51:68-80.

de Reus MA & van den Heuvel MP. 2013. The parcellation-based connectome: limitations and extensions. *Neuroimage*. 80:397-404.

Desikan RS, Segonne F, Fischl B, Quinn BT, Dickerson BC, Blacker D, Buckner RL, Dale AM, Maguire RP, Hyman BT, Albert MS & Killiany RJ. 2006. An automated labeling system for subdividing the human cerebral cortex on MRI scans into gyral based regions of interest. *Neuroimage*. 31:968-980.

Dixon ML, Moodie CA, Goldin PR, Farb N, Heimberg RG & Gross JJ. 2020. Emotion Regulation in Social Anxiety Disorder: Reappraisal and Acceptance of Negative Self-beliefs. *Biol Psychiatry Cogn Neurosci Neuroimaging*. 5:119-129.

Ducharme S, Albaugh MD, Nguyen TV, Hudziak JJ, Mateos-Perez JM, Labbe A, Evans AC, Karama S & Grp BDC. 2015. Trajectories of cortical surface area and cortical volume maturation in normal brain development. *Data in Brief*. 5:929-938.

Etkin A. 2012. Neurobiology of Anxiety: From Neural Circuits to Novel Solutions? *Depression and Anxiety*. 29:355-358.

Etkin A. 2019. A Reckoning and Research Agenda for Neuroimaging in Psychiatry. *Am J Psychiatry*. 176:507-511.

Etkin A, Egner T & Kalisch R. 2011. Emotional processing in anterior cingulate and medial prefrontal cortex. *Trends in Cognitive Sciences*. 15:85-93.

Etkin A & Wager TD. 2007. Functional neuroimaging of anxiety: a meta-analysis of emotional processing in PTSD, social anxiety disorder, and specific phobia. *Am J Psychiatry*. 164:1476-88.

Evans AC. 2013. Networks of anatomical covariance. *Neuroimage*. 80:489-504.

Faul F, Erdfelder E, Lang AG & Buchner A. 2007. G*Power 3: a flexible statistical power analysis program for the social, behavioral, and biomedical sciences. *Behav Res Methods*. 39:175-91.

Finn ES, Scheinost D, Finn DM, Shen X, Papademetris X & Constable RT. 2017. Can brain state be manipulated to emphasize individual differences in functional connectivity? *Neuroimage*. 160:140-151.

Fischl B & Dale AM. 2000a. Measuring the thickness of the human cerebral cortex from magnetic resonance images. *Proceedings of the National Academy of Sciences of the United States of America*. 97:11050-11055.

Fischl B & Dale AM. 2000b. Measuring the thickness of the human cerebral cortex from magnetic resonance images. *Proc Natl Acad Sci U S A*. 97:11050-5.

Fischl B, Salat DH, Busa E, Albert M, Dieterich M, Haselgrove C, van der Kouwe A, Killiany R, Kennedy D, Klaveness S, Montillo A, Makris N, Rosen B & Dale AM. 2002. Whole brain segmentation: Automated labeling of neuroanatomical structures in the human brain. *Neuron*. 33:341-355.

Fischl B, Sereno MI & Dale AM. 1999. Cortical surface-based analysis. II: Inflation, flattening, and a surface-based coordinate system. *Neuroimage*. 9:195-207.

Fischl B, van der Kouwe A, Destrieux C, Halgren E, Segonne F, Salat DH, Busa E, Seidman LJ, Goldstein J, Kennedy D, Caviness V, Makris N, Rosen B & Dale AM. 2004. Automatically parcellating the human cerebral cortex. *Cerebral Cortex*. 14:11-22.

Frick A, Gingnell M, Marquand AF, Howner K, Fischer H, Kristiansson M, Williams SC, Fredrikson M & Furmark T. 2014. Classifying social anxiety disorder using multivoxel pattern analyses of brain function and structure. *Behav Brain Res*. 259:330-5.

Genovese CR, Lazar NA & Nichols T. 2002. Thresholding of statistical maps in functional neuroimaging using the false discovery rate. *Neuroimage*. 15:870-8.

Gentili C, Cristea IA, Angstadt M, Klumpp H, Tozzi L, Phan KL & Pietrini P. 2016. Beyond emotions: A meta-analysis of neural response within face processing system in social anxiety. *Experimental Biology and Medicine*. 241:225-237.

Girard G, Whittingstall K, Deriche R & Descoteaux M. 2014. Towards quantitative connectivity analysis: reducing tractography biases. *Neuroimage*. 98:266-78.

Goldin PR, Manber T, Hakimi S, Canli T & Gross JJ. 2009. Neural bases of social anxiety disorder: emotional reactivity and cognitive regulation during social and physical threat. *Arch Gen Psychiatry*. 66:170-80.

Gong G, He Y, Chen ZJ & Evans AC. 2012. Convergence and divergence of thickness correlations with diffusion connections across the human cerebral cortex. *Neuroimage*. 59:1239-48.

Groenewold NA, Bas-Hoogendam JM, Amod AR, Laansma MA, Van Velzen LS, Aghajani M, Hilbert K, Oh H, Salas R, Jackowski AP, Pan PM, Salum GA, Blair JR, Blair KS, Hirsch J, Pantazatos SP, Schneier FR, Talati A, Roelofs K, Volman I, Blanco-Hinojo L, Cardoner N, Pujol J, Beesdo-Baum K, Ching CRK, Thomopoulos SI, Jansen A, Kircher T, Krug A, Nenadić I, Stein F, Dannlowski U, Grotegerd D, Lemke H, Meinert S, Winter A, Erb M, Kreifelts B, Gong Q, Lui S, Zhu F, Mwangi B, Soares JC, Wu MJ, Bayram A, Canli M, Tükel R, Westenberg PM, Heeren A, Cremers HR, Hofmann D, Straube T, Doruyter AGG, Lochner C, Peterburs J, Van Tol MJ, Gur RE, Kaczkurkin AN, Larsen B, Satterthwaite TD, Filippi CA, Gold AL, Harrewijn A, Zugman A, Bülow R, Grabe HJ, Völzke H, Wittfeld K, Böhnlein J, Dohm K, Kugel H, Schrammen E, Zwanzger P, Leehr EJ, Sindermann L, Ball TM, Fonzo GA, Paulus MP, Simmons A, Stein MB, Klumpp H, Phan KL, Furmark T, Månsson KNT, Manzouri A, Avery SN, Blackford JU, Clauss JA, Feola B, Harper JC, Sylvester CM, Lueken U, Veltman DJ, Winkler AM, Jahanshad N, Pine DS, Thompson PM, Stein DJ & Van der

Wee NJA. 2023. Volume of subcortical brain regions in social anxiety disorder: mega-analytic results from 37 samples in the ENIGMA-Anxiety Working Group. *Mol Psychiatry*. 28:1079-1089.

Hardee JE, Cope LM, Munier EC, Welsh RC, Zucker RA & Heitzeg MM. 2017. Sex differences in the development of emotion circuitry in adolescents at risk for substance abuse: a longitudinal fMRI study. *Soc Cogn Affect Neurosci*. 12:965-975.

He Y, Chen Z & Evans A. 2008. Structural insights into aberrant topological patterns of large-scale cortical networks in Alzheimer's disease. *J Neurosci*. 28:4756-66.

He Y, Chen ZJ & Evans AC. 2007. Small-world anatomical networks in the human brain revealed by cortical thickness from MRI. *Cereb Cortex*. 17:2407-19.

He Y & Zhang M. 2004. Study on reliability and validity of the Liebowitz Social Anxiety Scale. *Journal of Diagnostics Concepts & Practice*. 3:89-93.

Hiser J & Koenigs M. 2018. The Multifaceted Role of the Ventromedial Prefrontal Cortex in Emotion, Decision Making, Social Cognition, and Psychopathology. *Biol Psychiatry*. 83:638-647.

Hogstrom LJ, Westlye LT, Walhovd KB & Fjell AM. 2013. The structure of the cerebral cortex across adult life: age-related patterns of surface area, thickness, and gyrification. *Cereb Cortex*. 23:2521-30.

Homan P, Argyelan M, DeRosse P, Szeszko PR, Gallego JA, Hanna L, Robinson DG, Kane JM, Lencz T & Malhotra AK. 2019. Structural similarity networks predict clinical outcome in early-phase psychosis. *Neuropsychopharmacology*. 44:915-922.

Janak PH & Tye KM. 2015. From circuits to behaviour in the amygdala. *Nature*. 517:284-92.

Kong XZ, Liu Z, Huang L, Wang X, Yang Z, Zhou G, Zhen Z & Liu J. 2015. Mapping Individual Brain Networks Using Statistical Similarity in Regional

Morphology from MRI. *PLoS One*. 10:e0141840.

Kong XZ, Wang X, Huang L, Pu Y, Yang Z, Dang X, Zhen Z & Liu J. 2014. Measuring individual morphological relationship of cortical regions. *J Neurosci Methods*. 237:103-7.

Kreifelts B, Eckstein KN, Ethofer T, Wiegand A, Wächter S, Brück C, Erb M, Lotze M & Wildgruber D. 2019. Tuned to voices and faces: Cerebral responses linked to social anxiety. *Neuroimage*. 197:450-456.

Kreifelts B, Ethofer T, Wiegand A, Brück C, Wächter S, Erb M, Lotze M & Wildgruber D. 2020. The Neural Correlates of Face-Voice-Integration in Social Anxiety Disorder. *Front Psychiatry*. 11:657.

Kriegeskorte N, Simmons WK, Bellgowan PS & Baker CI. 2009. Circular analysis in systems neuroscience: the dangers of double dipping. *Nat Neurosci*. 12:535-40.

Kropf E, Syan SK, Minuzzi L & Frey BN. 2019. From anatomy to function: the role of the somatosensory cortex in emotional regulation. *Braz J Psychiatry*. 41:261-269.

Lai H, Kong X, Zhao Y, Pan N, Zhang X, He M, Wang S & Gong Q. 2022. Patterns of a structural covariance network associated with dispositional optimism during late adolescence. *Neuroimage*. 251:119009.

Latora V & Marchiori M. 2001. Efficient behavior of small-world networks. *Phys Rev Lett*. 87:198701.

Lei D, Li W, Tallman MJ, Patino LR, McNamara RK, Strawn JR, Klein CC, Nery FG, Fleck DE, Qin K, Ai Y, Yang J, Zhang W, Lui S, Gong Q, Adler CM, Sweeney JA & DelBello MP. 2021. Changes in the brain structural connectome after a prospective randomized clinical trial of lithium and quetiapine treatment in youth with bipolar disorder. *Neuropsychopharmacology*. 46:1315-1323.

Lei D, Li W, Tallman MJ, Strakowski SM, DelBello MP, Rodrigo Patino L, Fleck DE,

Lui S, Gong Q, Sweeney JA, Strawn JR, Nery FG, Welge JA, Rummelhoff E & Adler CM. 2022. Changes in the structural brain connectome over the course of a nonrandomized clinical trial for acute mania. *Neuropsychopharmacology*.

Li Y, Wang N, Wang H, Lv Y, Zou Q & Wang J. 2021. Surface-based single-subject morphological brain networks: Effects of morphological index, brain parcellation and similarity measure, sample size-varying stability and test-retest reliability. *Neuroimage*. 235:118018.

Liao X, Vasilakos AV & He Y. 2017. Small-world human brain networks: Perspectives and challenges. *Neurosci Biobehav Rev*. 77:286-300.

Liu F, Guo W, Fouche JP, Wang Y, Wang W, Ding J, Zeng L, Qiu C, Gong Q, Zhang W & Chen H. 2015. Multivariate classification of social anxiety disorder using whole brain functional connectivity. *Brain Struct Funct*. 220:101-15.

Liu Z, Palaniyappan L, Wu X, Zhang K, Du J, Zhao Q, Xie C, Tang Y, Su W, Wei Y, Xue K, Han S, Tsai SJ, Lin CP, Cheng J, Li C, Wang J, Sahakian BJ, Robbins TW, Zhang J & Feng J. 2021. Resolving heterogeneity in schizophrenia through a novel systems approach to brain structure: individualized structural covariance network analysis. *Mol Psychiatry*. 26:7719-7731.

Marek R, Strobel C, Bredy TW & Sah P. 2013. The amygdala and medial prefrontal cortex: partners in the fear circuit. *J Physiol*. 591:2381-91.

Maslov S & Sneppen K. 2002. Specificity and stability in topology of protein networks. *Science*. 296:910-3.

Meier SM, Petersen L, Mattheisen M, Mors O, Mortensen PB & Laursen TM. 2015. Secondary depression in severe anxiety disorders: a population-based cohort study in Denmark. *Lancet Psychiatry*. 2:515-523.

Mennin DS, Fresco DM, Heimberg RG, Schneier FR, Davies SO & Liebowitz MR.

2002. Screening for social anxiety disorder in the clinical setting: using the Liebowitz Social Anxiety Scale. *Journal of Anxiety Disorders*. 16:661-673.

Mizzi S, Pedersen M, Lorenzetti V, Heinrichs M & Labuschagne I. 2022. Resting-state neuroimaging in social anxiety disorder: a systematic review. *Mol Psychiatry*. 27:164-179.

Montembeault M, Joubert S, Doyon J, Carrier J, Gagnon JF, Monchi O, Lungu O, Belleville S & Brambati SM. 2012. The impact of aging on gray matter structural covariance networks. *Neuroimage*. 63:754-9.

Niu R, Lei D, Chen F, Chen Y, Suo X, Li L, Lui S, Huang X, Sweeney JA & Gong Q. 2018. Reduced local segregation of single-subject gray matter networks in adult PTSD. *Hum Brain Mapp*. 39:4884-4892.

Ochsner KN, Silvers JA & Buhle JT. 2012. Functional imaging studies of emotion regulation: a synthetic review and evolving model of the cognitive control of emotion. *Ann N Y Acad Sci*. 1251:E1-24.

Palaniyappan L, Mallikarjun P, Joseph V, White TP & Liddle PF. 2011. Regional contraction of brain surface area involves three large-scale networks in schizophrenia. *Schizophrenia Research*. 129:163-168.

Penninx BW, Pine DS, Holmes EA & Reif A. 2021. Anxiety disorders. *Lancet*. 397:914-927.

Pourtois G, Sander D, Andres M, Grandjean D, Reveret L, Olivier E & Vuilleumier P. 2004. Dissociable roles of the human somatosensory and superior temporal cortices for processing social face signals. *Eur J Neurosci*. 20:3507-15.

Qiu L, Lui S, Kuang W, Huang X, Li J, Li J, Zhang J, Chen H, Sweeney JA & Gong Q. 2014. Regional increases of cortical thickness in untreated, first-episode major depressive disorder. *Transl Psychiatry*. 4:e378.

Raichle ME. 2015. The brain's default mode network. *Annu Rev Neurosci*. 38:433-47.

Rakic P. 1988. Specification of Cerebral Cortical Areas. *Science*. 241:170-176.

Rashid B & Calhoun V. 2020. Towards a brain-based predictome of mental illness. *Hum Brain Mapp*. 41:3468-3535.

Ren Y, Guo L & Guo CC. 2019. A connectivity-based parcellation improved functional representation of the human cerebellum. *Sci Rep*. 9:9115.

Reuter M, Schmansky NJ, Rosas HD & Fischl B. 2012. Within-subject template estimation for unbiased longitudinal image analysis. *Neuroimage*. 61:1402-1418.

Rubinov M & Sporns O. 2010. Complex network measures of brain connectivity: uses and interpretations. *Neuroimage*. 52:1059-69.

Ruscio AM, Brown TA, Chiu WT, Sareen J, Stein MB & Kessler RC. 2008. Social fears and social phobia in the USA: results from the National Comorbidity Survey Replication. *Psychological Medicine*. 38:15-28.

Sanabria-Diaz G, Melie-García L, Iturria-Medina Y, Alemán-Gómez Y, Hernández-González G, Valdés-Urrutia L, Galán L & Valdés-Sosa P. 2010. Surface area and cortical thickness descriptors reveal different attributes of the structural human brain networks. *Neuroimage*. 50:1497-510.

Sarwar T, Ramamohanarao K & Zalesky A. 2019. Mapping connectomes with diffusion MRI: deterministic or probabilistic tractography? *Magn Reson Med*. 81:1368-1384.

Seidlitz J, Váša F, Shinn M, Romero-Garcia R, Whitaker KJ, Vértes PE, Wagstyl K, Kirkpatrick Reardon P, Clasen L, Liu S, Messinger A, Leopold DA, Fonagy P, Dolan RJ, Jones PB, Goodyer IM, Raznahan A & Bullmore ET. 2018. Morphometric Similarity Networks Detect Microscale Cortical Organization and Predict Inter-Individual Cognitive Variation. *Neuron*. 97:231-247.e7.

Sergerie K, Chochol C & Armony JL. 2008. The role of the amygdala in emotional processing: a quantitative meta-analysis of functional neuroimaging studies. *Neurosci Biobehav Rev*. 32:811-30.

Sharda M, Khundrakpam BS, Evans AC & Singh NC. 2016. Disruption of structural covariance networks for language in autism is modulated by verbal ability. *Brain Struct Funct*. 221:1017-32.

Singh MK, Kesler SR, Hadi Hosseini SM, Kelley RG, Amatya D, Hamilton JP, Chen MC & Gotlib IH. 2013. Anomalous gray matter structural networks in major depressive disorder. *Biol Psychiatry*. 74:777-85.

Singh SP, Cooper JE, Fisher HL, Tarrant CJ, Lloyd T, Banjo J, Corfe S & Jones P. 2005. Determining the chronology and components of psychosis onset: The Nottingham Onset Schedule (NOS). *Schizophr Res*. 80:117-30.

Sporns O, Tononi G & Kötter R. 2005. The human connectome: A structural description of the human brain. *PLoS Comput Biol*. 1:e42.

Sporns O & Zwi JD. 2004. The small world of the cerebral cortex. *Neuroinformatics*. 2:145-62.

Stein MB & Stein DJ. 2008. Social anxiety disorder. *Lancet*. 371:1115-1125.

Storsve AB, Fjell AM, Tamnes CK, Westlye LT, Overbye K, Aasland HW & Walhovd KB. 2014. Differential Longitudinal Changes in Cortical Thickness, Surface Area and Volume across the Adult Life Span: Regions of Accelerating and Decelerating Change. *Journal of Neuroscience*. 34:8488-8498.

Strogatz SH. 2001. Exploring complex networks. *Nature*. 410:268-76.

Suo XS, Lei DL, Li LL, Li WL, Dai JD, Wang SW, He MH, Zhu HZ, Kemp GJK & Gong QG. 2018. Psychoradiological patterns of small-world properties and a systematic review of connectome studies of patients with 6 major psychiatric

disorders. *J Psychiatry Neurosci*. 43:427.

Sylvester CM, Corbetta M, Raichle ME, Rodebaugh TL, Schlaggar BL, Sheline YI, Zorumski CF & Lenze EJ. 2012. Functional network dysfunction in anxiety and anxiety disorders. *Trends Neurosci*. 35:527-35.

Talati A, Pantazatos SP, Schneier FR, Weissman MM & Hirsch J. 2013. Gray matter abnormalities in social anxiety disorder: primary, replication, and specificity studies. *Biol Psychiatry*. 73:75-84.

Tamnes CK, Herting MM, Goddings AL, Meuwese R, Blakemore SJ, Dahl RE, Gueroglu B, Raznahan A, Sowell ER, Crone EA & Mills XL. 2017. Development of the Cerebral Cortex across Adolescence: A Multisample Study of Inter-Related Longitudinal Changes in Cortical Volume, Surface Area, and Thickness. *Journal of Neuroscience*. 37:3402-3412.

Tijms BM, Seriès P, Willshaw DJ & Lawrie SM. 2012. Similarity-based extraction of individual networks from gray matter MRI scans. *Cereb Cortex*. 22:1530-41.

Turner GR & Spreng RN. 2012. Executive functions and neurocognitive aging: dissociable patterns of brain activity. *Neurobiol Aging*. 33:826.e1-13.

Tzourio-Mazoyer N, Landeau B, Papathanassiou D, Crivello F, Etard O, Delcroix N, Mazoyer B & Joliot M. 2002. Automated anatomical labeling of activations in SPM using a macroscopic anatomical parcellation of the MNI MRI single-subject brain. *Neuroimage*. 15:273-89.

Van Erven T & Harrëmos P. 2014. Rényi divergence and kullback-leibler divergence. *IEEE Transactions on Information Theory*. 60:3797-3820.

Wang H, Jin X, Zhang Y & Wang J. 2016. Single-subject morphological brain networks: connectivity mapping, topological characterization and test-retest reliability. *Brain Behav*. 6:e00448.

Wang J, Wang X, Xia M, Liao X, Evans A & He Y. 2015. GRETNA: a graph theoretical network analysis toolbox for imaging connectomics. *Front Hum Neurosci*. 9:386.

Watts DJ & Strogatz SH. 1998. Collective dynamics of 'small-world' networks. *Nature*. 393:440-2.

Yang H, Chen X, Chen ZB, Li L, Li XY, Castellanos FX, Bai TJ, Bo QJ, Cao J, Chang ZK, Chen GM, Chen NX, Chen W, Cheng C, Cheng YQ, Cui XL, Duan J, Fang Y, Gong QY, Guo WB, Hou ZH, Hu L, Kuang L, Li F, Li HX, Li KM, Li T, Liu YS, Liu ZN, Long YC, Lu B, Luo QH, Meng HQ, Peng D, Qiu HT, Qiu J, Shen YD, Shi YS, Si TM, Tang YQ, Wang CY, Wang F, Wang K, Wang L, Wang X, Wang Y, Wang YW, Wu XP, Wu XR, Xie CM, Xie GR, Xie HY, Xie P, Xu XF, Yang J, Yao JS, Yao SQ, Yin YY, Yuan YG, Zang YF, Zhang AX, Zhang H, Zhang KR, Zhang L, Zhang ZJ, Zhao JP, Zhou R, Zhou YT, Zhu JJ, Zhu ZC, Zou CJ, Zuo XN & Yan CG. 2021. Disrupted intrinsic functional brain topology in patients with major depressive disorder. *Mol Psychiatry*. 26:7363-7371.

Yang X, Liu J, Meng Y, Xia M, Cui Z, Wu X, Hu X, Zhang W, Gong G, Gong Q, Sweeney JA & He Y. 2019. Network analysis reveals disrupted functional brain circuitry in drug-naive social anxiety disorder. *Neuroimage*. 190:213-223.

Yun JY, Boedhoe PSW, Vriend C, Jahanshad N, Abe Y, Ameis SH, Anticevic A, Arnold PD, Batistuzzo MC, Benedetti F, Beucke JC, Bollettini I, Bose A, Brem S, Calvo A, Cheng Y, Cho KIK, Ciullo V, Dallaspezia S, Denys D, Feusner JD, Fouche JP, Giménez M, Gruner P, Hibar DP, Hoexter MQ, Hu H, Huyser C, Ikari K, Kathmann N, Kaufmann C, Koch K, Lazaro L, Lochner C, Marques P, Marsh R, Martínez-Zalacaín I, Mataix-Cols D, Menchón JM, Minuzzi L, Morgado P, Moreira P, Nakamae T, Nakao T, Narayanaswamy JC, Nurmi EL, O'Neill J, Piacentini J, Piras F, Piras F, Reddy YCJ, Sato JR, Simpson HB, Soreni N, Soriano-Mas C, Spalletta G, Stevens MC, Szeszko PR, Tolin DF, Venkatasubramanian G, Walitza S, Wang Z, van

Wingen GA, Xu J, Xu X, Zhao Q, Thompson PM, Stein DJ, van den Heuvel OA & Kwon JS. 2020. Brain structural covariance networks in obsessive-compulsive disorder: a graph analysis from the ENIGMA Consortium. *Brain*. 143:684-700.

Zalesky A, Cocchi L, Fornito A, Murray MM & Bullmore E. 2012. Connectivity differences in brain networks. *Neuroimage*. 60:1055-62.

Zhan Y, Wei J, Liang J, Xu X, He R, Robbins TW & Wang Z. 2021. Diagnostic Classification for Human Autism and Obsessive-Compulsive Disorder Based on Machine Learning From a Primate Genetic Model. *Am J Psychiatry*. 178:65-76.

Zhang X, Cheng B, Yang X, Suo X, Pan N, Chen T, Wang S & Gong Q. 2022a. Emotional intelligence mediates the protective role of the orbitofrontal cortex spontaneous activity measured by fALFF against depressive and anxious symptoms in late adolescence. *Eur Child Adolesc Psychiatry*.

Zhang X, Luo Q, Wang S, Qiu L, Pan N, Kuang W, Lui S, Huang X, Yang X, Kemp GJ & Gong Q. 2020. Dissociations in cortical thickness and surface area in non-comorbid never-treated patients with social anxiety disorder. *EBioMedicine*. 58:102910.

Zhang X, Suo X, Yang X, Lai H, Pan N, He M, Li Q, Kuang W, Wang S & Gong Q. 2022b. Structural and functional deficits and couplings in the cortico-striato-thalamo-cerebellar circuitry in social anxiety disorder. *Transl Psychiatry*. 12:26.

Zugman A, Winkler AM & Pine DS. 2021. Recent advances in understanding neural correlates of anxiety disorders in children and adolescents. *Curr Opin Psychiatry*. 34:617-623.